

Densely packed rectangulations

R Krishnamurti

Department of Architecture, Carnegie Mellon University, Pittsburgh, PA 15213, USA;
e-mail: ramesh@arc.cmu.edu

C F Earl

Department of Mechanical, Materials and Manufacturing Engineering, University of Newcastle upon Tyne, Newcastle upon Tyne NE1 7RU, England; e-mail: C.F.Earl@ncl.ac.uk

Received 8 March 1997; in revised form 16 May 1998

Abstract. Rectangulations include packings of rectangles in two dimensions and packings of cuboids (3-rectangles) in three dimensions. Spatial layouts of this type are used in architectural and engineering design. In this paper we examine the spatial relations between the lines, planes, and volume elements in these designs. It is shown how to describe rectangulations as shapes in product algebras. Spatial relations, particularly adjacencies between areas, volumes, maximal planes, or maximal lines are used to represent rectangulations. More general properties of these spatial relations are derived. Generative properties of rectangulations are established which distinguish those 3-rectangulations which have an essentially two-dimensional character.

Introduction

Three-dimensional rectangulations or 3-rectangulations are arrangements of rectangular volumes or cuboids (3-rectangles). The boundaries of the 3-rectangles are aligned along mutually perpendicular directions. For densely packed rectangulations the 3-rectangles do not overlap, there are no gaps between them, and they are packed into a 3-rectangle. The boundary faces of 3-rectangles join to form maximal planes. The joints among the maximal planes classify types of 3-rectangulation (Earl, 1978). In Krishnamurti (1979) classes of 3-rectangulations are generated on a cellular grid by distinguishing rules for the occupancy of grid cells. Densely packed rectangulations are part of a wider class of shapes consisting of loosely packed arrangements of rectangles (Flemming, 1986). Two-dimensional rectangulations (2-rectangulations) are called rectangular dissections (Steadman, 1983).

Rectangulations, both loosely and densely packed, have served as a formally defined class of spatial configurations representing layout designs in two and three dimensions. In examples from architectural design (Flemming, 1986; Steadman, 1983) the rectangular areas are treated as spaces and their boundary lines as walls. In these examples rectangulations have two distinct applications. First, as a formally defined class of geometrical configurations of a floor-plan layout type. Second, as a representative sample from which other layouts can be derived by local modifications such as taking the shape sum of adjacent rectangles or subdividing large rectangular areas. There are several ways of generating these rectangular configurations by grammars (Earl, 1980; Krishnamurti, 1979). A family of similar grammars specifies a wider class of rectangular shapes. Flemming's treatment of loosely packed rectangulations (Flemming, 1986; 1989) and their construction in the LOOS system provides a comprehensive framework for describing and generating spatial layouts. The LOOS implementation has been applied to aid the evaluation of different search methods in design applications (Flemming et al, 1992) and as a component in a conceptual building design demonstrator (Flemming and Chien, 1995).

Layout design is a component in many areas of design, including architecture, mechanical and electromechanical engineering, electronics, and building construction. The architectural sources for the study of rectangular spatial layouts have been outlined above. Spatial layouts in engineering design are now considered. It may be instructive to distinguish two ways in which spatial layouts have been generated in engineering applications. First, spatial elements or 'pixel-like' areas or volumes are aggregated to form functional spaces. Rules incrementally modify spaces to meet shape and functional criteria. In an example of this approach applied to complex engineer-to-order (that is, one-of-a-kind) products, such as oil-platform topside layout (Smith et al, 1996), an expert system is used to generate associativity data (Chao et al, 1997) specifying the relationships among spaces and a simulated annealing algorithm to optimise layout. A characteristic of this approach is that intermediate configurations generated in the process of searching for a layout range freely under the constraints of the rules.

Second, functional spatial elements are composed by rules to generate possible designs. An example is the problem of three-dimensional component packing for design applications (Szykman and Cagan, 1995). A distinction is made between constrained and unconstrained problems. The constrained problem (Szykman and Cagan, 1997) corresponds to design applications where associativities and space attributes need to be satisfied as well as optimising the layout against an objective function. The search for suitable designs within the rule framework again uses simulated annealing (Cagan and Mitchell, 1993). An advantage of simulated annealing for layout problems is that it is possible to move out of the space of valid layouts during the search. As penalties are incurred for invalid layouts, such as those with overlaps among spaces, the process tends towards final valid layouts. Other examples of this approach include the design of machine layouts (Hicks et al, 1994) generated as loosely packed rectangulations, three-dimensional manufacturing layouts of process, transfer, and handling equipment, construction site layout (Choi and Flemming, 1996), and electronic component packing (Campbell et al, 1997).

Electronic circuit layout is an engineering domain in which rectangular elements are widely used. The boundaries of adjacent rectangles represent channels through which connections between components located in the rectangles are made. In contrast to the architectural and mechanical examples the layout problem shifts from concentration on rectangular spaces to the configuration of boundaries, whether lines or planes (Preas and van Cleemput, 1979; Supowit and Slutz, 1984). The wall representations of Flemming (1978; 1980) are directly applicable to these examples, and formal results on the equivalence of region and wall representations are presented by Kundu (1988). A boundary view of rectangulations is used later in this paper to describe underlying constraints and freedoms in the design of three-dimensional spatial layouts.

This investigation of 3-rectangulations is motivated by two general aims. First, to try to understand the geometrical properties of fully three-dimensional configurations arising in applications such as architecture, electronics, factory layouts, and compact equipment packing in aerospace or consumer electronics. In these examples small dimensional changes can lead to a cascade of configurational alterations yielding a functionally unsuitable design. CAD geometric modelling provides tools for constructing volume and surface elements and combining them into compositions. The CAD tools display the results of compositions (and construct associated geometric models) but spatial analysis is largely left to the designer. The designer's expertise and knowledge of the problem domain controls and guides spatial composition. CAD tools help visualisation, clash detection, and occupancy analysis of a proposed design.

Second, rectangulations present an example of a class of shapes for which different descriptions in terms of shape elements (volumes and boundary planes) are used

simultaneously in design applications. The 3-rectangulations offer a class of shapes in which descriptions can be examined individually and in combination. Formal specification of descriptions yields data structures. For 2-rectangulations, data structures based on generative schemes (Krishnamurti, 1979; Kundu, 1988) have provided computational mechanisms for manipulating the shapes.

In this paper we are not defining an approach to spatial layout problems; rather we consider how layouts are described as shapes and spatial relations. Three-dimensional layouts display a wide variety of possible configurations. However, these configurations are constrained by geometric conditions placed on the elements and relations, such as rectangularity and dense packing. We examine how these constraints affect possible configurations and their resulting properties. These properties range from the local properties at joints in densely packed 3-rectangulations (Earl, 1978) to the more global ones of spatial relations among shape elements across the configuration.

Maximal plane adjacency (one of the spatial relations between elements) is used by Krishnamurti (1993) to represent unlocked trivalent 3-rectangulations. This class of 3-rectangulations is identified by the condition that maximal planes are rectangles which do not cross one another. The maximal plane adjacency representation is not appropriate for other classes of 3-rectangulation. These require more information on the properties of maximal planes and the types of adjacencies. We show how to characterise those 3-dimensional maps which are maximal plane adjacency descriptions of unlocked trivalent 3-rectangulations. These descriptions can thus support shape computations on rectangulations. Changes that occur in the rectangulations (at least configurational changes) are reflected in corresponding changes in the maximal plane adjacency description. We are not making special claims for a limited class of three-dimensional layouts but use them to: (a) indicate the properties of more complex classes; (b) provide an example of different spatial descriptions of a spatial configuration; (c) develop formal representations of the class.

The analysis of rectangulations also provides an example of the ways in which shapes are described by elements (Earl, 1997; Stouffs, 1994). Some preliminary definitions are given here. Elements are defined by descriptors and boundaries. Descriptors define lines, planes, or volumes, and the boundaries locate the element segments. A shape S is described by selected elements $E(S)$. An element x in $E(S)$ has boundary $b(x)$. Elements with equal descriptors can be combined by finite sums and products to form new elements $E'(S)$. Subsets X of $E'(S)$ which cover S can be used to describe S , with associated boundaries $b(X)$ formed from the shape sum of the elements X . Among the subsets describing S , there is one for which the boundary is minimal. It is associated with the maximal elements in $E'(S)$.

The properties of 3-rectangulations depend critically on the properties of 2-rectangulations because cross sections of 3-rectangulations are 2-rectangulations. Descriptions and properties of densely packed 2-rectangulations will be reviewed for application to the dimensional case. In the following we assume that all rectangulations are densely packed.

2-rectangulations as shapes

A 2-rectangulation R_{22} in shape algebra U_{22} (Stiny, 1991) is described by a set of rectangular plane elements E_{22} . A shape algebra U_{ij} has shapes of dimension i embedded in a space of dimension j . For example, U_{22} contains coplanar plane elements and U_{23} contains general plane elements embedded in three dimensions. The notation E_{22} indicates that these elements are in shape algebra U_{22} . For x, y in E_{22} , the shape product $x.y$ is empty (that is, the elements do not overlap). The shape sum, $\sum x$, of all elements x in E_{22} is a rectangular plane element (that is, the rectangles are densely packed into a rectangle).

Boundaries $b(x)$, of elements x in E_{22} , are rectangles, and minimal boundary $b^*(R_{22})$ is a rectangle (Earl, 1997). Trivalence is a property of boundaries. An element x is adjacent to y if $b(x).b(y)$ is not the empty shape. A rectangulation is trivalent if, for adjacent elements x and y , there are two elements which are each adjacent to x and y . An extended set of elements, formed from sums and products of elements in E_{22} , is denoted E'_{22} . These elements are not necessarily connected and represent collections of rectangles.

A 2-rectangulation R_{12} in shape algebra U_{12} is described by orthogonal maximal line elements M_{12} . These line elements have all boundary points coincident with other lines. There are four shared boundary points which identify a bounding rectangle. If, in addition, the incidence (Earl, 1997) and boundary of R_{12} (described by elements M_{12}) are equal, then the lines do not cross and R_{12} is trivalent.

The relation between the descriptions of rectangulations as lines and plane segments is now examined. If 2-rectangulation R_{22} is considered as a shape in U_{22} with elements E_{22} as above, then the boundary $b(e)$, e in E_{22} , is a rectangle. Boundary $b(e)$ has four maximal line segments. The set of line segments $\{b(e), e \text{ in } E_{22}\}$ can be used to describe a corresponding rectangulation R_{12} in U_{12} . Let the elements in this description be E_{12} . The sums and products of colinear elements in E_{12} yield elements E'_{12} . These elements are not necessarily connected and represent alignments across the rectangulation. The maximal element description M_{12} is constructed by using maximal connected elements in E'_{12} .

The two views of 2-rectangulations can be combined in a product description. Consider the rectangulation shape in $U_{12} \times U_{22}$ comprising a rectangulation R_{12} in U_{12} and a rectangulation R_{22} in U_{22} . The shapes R_{12} and R_{22} have element descriptions M_{12} and E_{22} , such that the boundary of R_{22} expressed as the sum of boundaries of elements in E_{22} equals the sum of elements in M_{12} . The shape $R_{12} \times R_{22}$ can be described by elements in the product set $M_{12} \times E_{22} = \{(m, e), m \text{ in } M_{12}, e \text{ in } E_{22}\}$. The description with elements M_{12} and E_{22} concentrates attention on combinations of lines across the shape, but leaving plane segments as discrete elements packed together. This view may overlook potential richness in the spatial structure emerging from combinations of the plane elements.

There are many alternative descriptions of a rectangulation in $U_{12} \times U_{22}$. We shall start with a description based on maximal lines and a single rectangular plane segment. The rectangulation is described by the product set of shape elements $\{(m, x), m \text{ in } M_{12}, x = \sum e, e \text{ in } E_{22}\}$. The U_{22} component of this product is not a rectangulation in its own right. It is by combination with the shapes in the U_{12} component that we obtain a rectangulation. This description of a rectangulation thus belongs properly to the product algebra. Further elements in U_{22} can be identified as elements in E'_{22} which are rectangles. These rectangles may be compositions of elements in E_{22} . The corresponding description of the rectangulation is the product set of shapes, $\{(m, e), m \text{ in } M_{12}, e \text{ in } E'_{22}, e \text{ is a rectangle}\}$. If we turn our attention to shape elements in U_{12} , other descriptions are $\{(e_{12}, e_{22}), e_{12} \text{ in } E_{12}, e_{22} \text{ in } E_{22}\}$, $\{(e'_{12}, e_{22}), e'_{12} \text{ in } E'_{12}, e_{22} \text{ in } E_{22}\}$, $\{(e_{12}, e'_{22}), e_{12} \text{ in } E_{12}, e'_{22} \text{ in } E'_{22}\}$, $\{(e'_{12}, e'_{22}), e'_{12} \text{ in } E'_{12}, e'_{22} \text{ in } E'_{22}\}$, and $\{(e_{12}, x), e_{12} \text{ in } E_{12}, x = \sum e, e \text{ in } E_{22}\}$. The use of elements E'_{22} widens the scope of the descriptions to include nonrectangular elements.

The subshapes used to describe a rectangulation in the product algebra $U_{12} \times U_{22}$ may not be set products of subshapes in U_{12} and in U_{22} . The subshapes may be formed by restricted pairs of subshapes. For example, subshapes composed from elements E_{22} and their associated boundaries (that is, rectangles and their boundaries taken together) can be used to describe a rectangulation in the product algebra $U_{12} \times U_{22}$. The U_{12} components in these restricted shapes are not shape elements. The relation between the

two components in this restricted subshape is not preserved under shape sum and shape product. For example, the product of two adjacent rectangles with boundary consists of the shape with components—the piece of shared boundary and the empty shape. These restricted subshapes are thus not candidates for closure algebras (Earl, 1997; Stiny, 1994) of subshapes in the product algebra. This description of a rectangulation illustrates the use of general descriptions based on selected subshapes rather than just shape elements.

Representation of 2-rectangulations

Densely packed 2-rectangulations are arrangements of nonoverlapping rectangles with a rectangular boundary. Trivalent 2-rectangulations are sections of trivalent unlocked 3-rectangulations. We will require the properties of 2-rectangulations to derive the spatial and generative characteristics of 3-rectangulations.

A trivalent 2-rectangulation is represented by a plane map of maximal line adjacency (Earl, 1980; Flemming, 1978). At an adjacency, one line abuts another. In Krishnamurti (1993) this asymmetry is included by directing the map edges. If line x abuts line y at an endpoint of x , then the corresponding edge (x, y) in the maximal line adjacency map has direction from x to y . The boundary face corresponding to the bounding rectangle is assigned bidirected edges, that is, edges with both directions.

Properties of maximal line adjacency maps arise immediately from the configuration of maximal lines in a trivalent 2-rectangulation.

- (a) All the faces are cycles of length 4, that is, the maps are quadrangulations (Brown, 1965). A cycle denotes a loop of incident edges and vertices, without regard to the directions on the edges. A directed cycle denotes that the edges have consistent directions around the loop.
- (b) There is a bidirected cycle of length 4. The length of a cycle is the number of vertices or edges it contains.
- (c) The out-degree of each vertex on the map is two. This means that each vertex has exactly two edges directed away from the vertex. This is denoted by $d^+(v) = 2$, where $d^+(v)$ is the out-degree, or number of edges directed away from, vertex v .
- (d) The map is 2-vertex coloured, that is, the vertices form two sets with each edge from a vertex in one set to a vertex in the other.
- (e) There are no multiple edges between vertices (that is, cycles of length 2).
- (f) The map is planar.

Let the directed quadrangulations satisfying all the conditions (a), (b), (c), (d), (e), and (f) be denoted by \mathbf{D} . We show that \mathbf{D} is precisely the set of maximal line adjacency maps of trivalent 2-rectangulations. We approach this result in two stages. First, we show that the quadrangulation property (a) is dependent on the other properties. Second, we construct these directed maps and interpret their construction in terms of rectangulations. Counting arguments relating the numbers of edges and faces of vertices are used frequently. Details of the counting arguments are shown in their first application but not subsequently.

For a plane map M satisfying conditions (b), (c), (d), (e), and (f), planarity gives $V - E + F = 2$ where V , E , and F denote the numbers of vertices, edges, and faces, respectively, in M . The out-degree condition gives $E = 2V - 4$, and edge counting gives $\sum iF_i = 2E$, where F_i denotes the number of faces with boundary cycle length i . These relations imply that $\sum (i - 4)F_i = 0$. There are no cycles of length 2 or 3, thus $F_2 = 0$ and $F_3 = 0$, and all faces have boundary cycle length 4. Thus M is a quadrangulation and satisfies condition (a).

The planarity condition (f) is important because planarity is not a consequence of the other properties (b), (c), (d), (e). As a counterexample, consider the 2-vertex

coloured graph with vertex sets $\{p, q, r, s\}$ and $\{1, 2, 3, 4\}$, and directed edges $\{(1, p), (1, r), (s, 1), (q, 2), (2, q), (r, 2), (2, r), (3, q), (q, 3), (3, r), (r, 3), (p, 3), (s, 3), (p, 4), (4, r), (4, s)\}$. This graph has bidirected cycle $(2, q, 3, r)$ and out-degree equal to two for all vertices, but is nonplanar because the subgraph on vertices $\{1, 3, 4, p, r, s\}$ is complete bipartite (Bondy and Murty, 1976).

In order to construct directed quadrangulations \mathbf{D} , some properties of cycles are identified. A cycle bounds a quadrangulation. Let us define an inward-directed edge as one from a vertex on the cycle to a vertex inside (where inside means away from the bidirected boundary). There is a simple relation between the length of the cycle and the number of inward-directed edges. This is established by counting arguments on the quadrangulation enclosed by the cycle, to give: *A cycle of length $2k$ in a directed quadrangulation in \mathbf{D} has $k-2$ inward-directed edges.*

A special case is: *Cycles of length 4 in directed quadrangulations in \mathbf{D} have no inward-directed edges.*

A nontrivial directed quadrangulation in \mathbf{D} has an internal vertex of degree 2 or 3 (by means of counting arguments). Removing a vertex of degree 2 retains a quadrangulation in \mathbf{D} (as there are no cycles of length 2) but with fewer vertices. Removing a vertex of degree 3 (planarity implies a surrounding cycle of length 6 if there are no vertices of degree 2) and its incident edges and replacing them with a single edge retains a directed quadrangulation in \mathbf{D} . The replacement can be chosen to maintain out-degree 2 vertices and to avoid creating a cycle of length 2. The properties of the inward-directed edges on cycles ensure this.

By reversing these operations, we can construct maps in \mathbf{D} with n vertices from those with $n - 1$ vertices. Corresponding rules (figure 1) construct 2-rectangulations. This establishes that: *Each directed quadrangulation in \mathbf{D} is the maximal line adjacency map of a 2-rectangulation.*

The argument leading to the result on generating directed quadrangulations in \mathbf{D} also shows that a quadrangulation without multiple edges [satisfying conditions (a) and (e)] can be assigned edge directions meeting conditions (b) and (c). This means that quadrangulations represent the underlying maximal line adjacency in 2-rectangulations.

Such a quadrangulation Q has a corresponding set of directed quadrangulations $D(Q)$ in \mathbf{D} . Each $D(Q)$ has in general many elements. This can be seen by reversing the directions in a directed cycle. Reversal retains all properties of a directed map in \mathbf{D} . Note that no directed cycles contain a boundary edge (except the boundary itself) because the boundary vertices have no inward-directed edges. These reversals of directed cycles generate all members in $D(Q)$ from one particular directed quadrangulation. This can be established by considering D_1 and D_2 in $D(Q)$. Consider edge (v, w) in Q with direction $w \rightarrow v$ in D_1 and direction $v \rightarrow w$ in D_2 . In D_2 there is an edge $w \rightarrow x$ with a corresponding directed edge $x \rightarrow w$ in D_1 . Repeating this operation creates a directed path v, w, x, \dots in D_2 and the corresponding reversed path $\dots x, w, v$

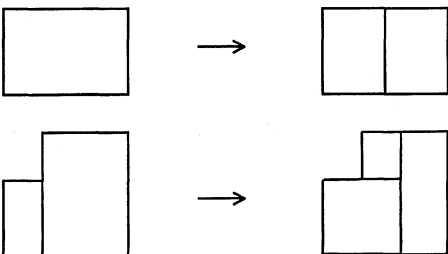


Figure 1. Rules for constructing 2-rectangulations.

in D_1 . The path in D_1 does not reach the bidirected boundary and is thus a directed cycle. Thus all edges on which directions can be reversed belong to directed cycles. Thus: *All directed quadrangulations in D with the same underlying quadrangulation can be derived from one another by sequences of reversals of directed cycles.*

The directed quadrangulations have connectivity properties based on directed paths. For a vertex v in a directed quadrangulation D in D , let us denote the maximal submap reached by directed paths from v by $C(v)$. The submap is also a directed quadrangulation in D . This follows from counting arguments and by noting that $C(v)$ reaches the bidirected boundary of the original quadrangulation (otherwise, the condition on in-directed edges on a cycle is violated). The faces of $C(v)$ can bound subquadrangulations in D so that $C(v)$ does not cover D completely but can miss out the subquadrangulations.

There are additional results for directed cycles in a directed quadrangulation in D . First, if there are no directed cycles (apart from the boundary) then there is a vertex of degree 2. This is established by following in reverse a directed path, against edge directions, until it terminates at an interior vertex (as there is no directed cycle), which has degree 2. Second, if there is a directed cycle (not the boundary) then there is a directed cycle of length 4. The directed cycle is either of length 4 or has an interior directed edge. Following this interior-directed edge, construct a 'smaller' directed cycle. Repeat the construction until a directed cycle of length 4 is found. In fact a stronger result holds for tracing back a path inside the cycle of length 4 against the edge directions (the original cycle is not a face) if either a vertex of degree 2 is found or, by repeating the construction, a directed cycle bounding a face is encountered. These two results are summarised as: *A directed quadrangulation in D contains either an interior face bounded by a directed cycle or a vertex of degree 2.*

A consequence is that rules in figure 1 for constructing 2-rectangulations may be simplified to splitting an existing rectangle or creating the 'pinwheel' rectangle corresponding to a directed cycle (figure 2).

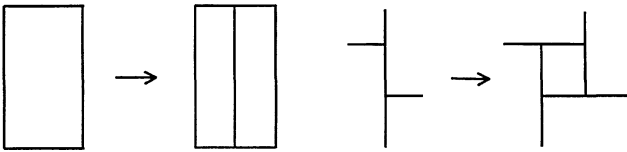


Figure 2. Simplified rules for constructing 2-rectangulations.

Similar results have been given in earlier papers on rectangulations. In particular, the last result on the existence of directed 4-cycles or a vertex of degree 2 was established by Supowit and Slutz (1984), in the context of cycles of connection paths in rectangular channels for VLSI design. The maximal line representation allows this result to be obtained economically and offers insights on the maximal line structure of 2-rectangulations.

To complete the review of 2-rectangulations we identify generation rules which are derived directly from the line configurations in the rectangulations. The mediation of the maximal line adjacency description is not always advantageous. Two types of rectangles occur in 2-rectangulations. These are illustrated in figure 3 (see over) as the right-hand sides of the corresponding rules for generating 2-rectangulations. The rules in figure 3 are of interest because at least one of them applies to each rectangle (Krishnamurti, 1993). For any labelling of the faces $\{f_i\}$ of a directed quadrangulation in D , there is an associated generation sequence which creates the faces in the same order, $f_1, f_2, f_3, \dots, f_n$.

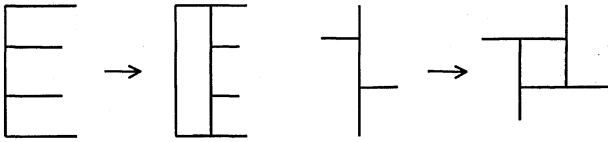


Figure 3. Rules for constructing 2-rectangulations with rectangles being added in any order.

3-rectangulations as shapes

A 3-rectangulation R_{33} in shape algebra U_{33} is a set of rectangular volumes (3-rectangles) E_{33} . For x, y in E_{33} , the shape product $x.y$ is empty (that is, the elements do not overlap). The shape sum, $\sum x$, of all elements x in E_{33} is a 3-rectangle giving a dense packing.

Boundaries $b(x)$, of elements x in E_{33} , are composed of 2-rectangles. The minimal boundary $b^*(R_{33})$ is similar. Trivalence is a property of boundaries. An element x is adjacent to y if $b(x).b(y)$ is not the empty shape. A 3-rectangulation is trivalent if, for adjacent elements x, y , and z , there are four 3-rectangles which are each adjacent to x, y , and z . An extended set of elements, formed from sums and products of elements in E_{33} , is denoted E'_{33} . These elements are not necessarily connected and represent collections of 3-rectangles.

A 3-rectangulation R_{23} in shape algebra U_{23} is described by orthogonal maximal plane elements M_{23} . These planes have all boundary lines coincident with boundaries of other planes and there are twelve shared boundary lines which identify a bounding 3-rectangle. If, in addition, the incidence and boundary of R_{23} (described by elements M_{23}) are equal, then the planes do not cross and R_{23} is trivalent.

If a 3-rectangulation R_{33} is considered as a shape in U_{33} with elements E_{33} as above, then the boundary $b(e)$, e in E_{33} , has six maximal plane segments. The set of plane segments in $\{b(e), e \text{ in } E_{33}\}$ can be used to form a description for a corresponding rectangulation R_{23} in U_{23} . Let the elements in this description be E_{23} . The sums and products of coplanar elements in E_{23} yield elements E'_{23} . These elements are not necessarily connected. The maximal element description M_{23} is constructed by using maximal connected elements in E'_{23} .

There are various descriptions of a rectangulation in $U_{23} \times U_{33}$ depending on the elements in U_{23} and U_{33} used to describe the shapes. One of these comprises a rectangulation R_{23} in U_{23} and a rectangulation R_{33} in U_{33} . An overall composite view composed of points, line planes, and volume elements is reviewed towards the end of the paper.

The subshapes used to describe a rectangulation in the product algebra $U_{23} \times U_{33}$ may be formed by restricted pairs of subshapes in U_{23} and U_{33} . For example, subshapes composed from elements E_{33} and their associated boundaries (that is, 3-rectangles and their boundaries taken together) can be used to describe a 3-rectangulation. However, as with the similar product shapes for 2-rectangulations, the selected shapes are not closed. For example, the shape product (that is, intersection) of two adjacent 3-rectangles with boundary consists of the shape with components—the shared rectangular plane segment and the empty shape which is not one of the shapes selected for the original description.

Unlocked trivalent 3-rectangulations

Maximal plane adjacency maps of unlocked trivalent 3-rectangulations (Krishnamurti, 1993) are three-dimensional maps. Each 3-face (that is, a three-dimensional face or 'volume') is an octahedron. Each face (or 2-face) is triangular and each edge (or 1-face) directed. The edges of the boundary octahedron are bidirected and each vertex has $d^+(v) = 4$.

There are two types of cycle of particular interest. First, the 1-cycles of edges are the conventional sequences of edges sharing endpoints. Second, the 2-cycles of triangular faces which form triangulated planar maps. These ‘topological’ 2-cycles have triangular faces edge to edge in pairs with no unpaired edges. There are no directed 1-cycles of length 3 and the maps are 3-vertex coloured. Lastly, there are exactly four triangular faces between the four out-directed edges at the vertex. Each of these faces contains two of the out-directed edges. This last property is denoted by $\delta^+(v) = 4$. Just as in the two-dimensional case, three-dimensional embedding is critical. In the following it is also assumed that there are no multiple edges or multiple 2-faces connecting the same vertices.

These properties are summarised in the following way. The maximal plane adjacency map of an unlocked trivalent 3-rectangulation is an edge-directed three-dimensional map with the following properties: (a) 3-faces octahedral; (b) 2-faces triangular; (c) boundary octahedron bidirected; (d) $d^+(v) = 4$ for all vertices; (e) $\delta^+(v) = 4$ for all vertices; (f) no directed 1-cycles of length 3; (g) no directed boundaries of triangular 2-faces; and (h) 3-vertex coloured.

There are dependencies among these properties. Condition (a) is dependent on the other conditions: $\{(b), (c), (d), (e), (h)\} \Rightarrow \{(a), (g)\}$, where a list of conditions indicates that they all hold. To establish this we use counting arguments.

Let V , E , F , and S denote the numbers of vertices, edges, 2-faces, and 3-faces. Euler’s relation gives $V - E + F - S = 0$. Conditions $d^+(v) = 4$ and $\delta^+(v) = 4$ yield $4V = E + 12$ and $4(V - 6) \leq F - 8$, respectively. The last inequality arises because four triangular faces are distinguished at each vertex by the $\delta^+(v) = 4$ condition. However, there may be triangular faces which are not counted in this way. Such faces have boundaries which are directed 1-cycles of length 3. This counting of triangular faces by use of the $\delta^+(v) = 4$ condition counts 2-faces at most once, and thus the inequality. Face counting gives $2F = \sum iS_i(F)$, where $S_i(F)$ is the number of 3-faces with i triangular faces. Together the above equations imply $\sum (i - 8)S_i(F) \leq 0$. Each 3-face has triangular 2-faces. The smallest which is 3-vertex coloured has eight faces, namely, the octahedron; thus $\sum (i - 8)S_i(F) \geq 0$. Therefore $\sum (i - 8)S_i(F) = 0$, and all 3-faces are octahedra. In addition, there are no triangular faces which are directed 3-cycles. The stronger result that there are no directed cycles of length 3 remains to be established later.

The previous result requires that $\delta^+(v) = 4$ and $d^+(v) = 4$. It appears that both these conditions are required to guarantee octahedral packing (all 3-faces octahedral). Now consider the conditions on which (e) [$\delta^+(v) = 4$] is dependent. By applying counting arguments similar to those above, we can establish the following dependencies: $\{(a), (c), (d), (g)\} \Rightarrow (e)$, and $\{(a), (c), (d), (e)\} \Rightarrow (g)$. Thus $\{(a), (c), (d), (g)\}$ is equivalent to $\{(a), (c), (d), (e)\}$. From these dependencies we get: $\{(a), (c), (d), (g)\}$ is equivalent to $\{(b), (c), (d), (e), (h)\}$.

Let T denote this class of three-dimensional directed octahedral maps specified by conditions $\{(a), (c), (d), (g)\}$ or $\{(b), (c), (d), (e), (h)\}$. We refer to these maps as octahedral because each of their 3-faces is an octahedron. We will now show that the directed octahedral maps T are the maximal plane adjacency maps of unlocked trivalent 3-rectangulations. First, the internal structure of elements in T is examined.

Consider T in T , and an internal vertex v of T . The vertices adjacent to v and the associated edges joining them form a quadrangulation $Q(v)$. Because $d^+(v) = 4$ and $\delta^+(v) = 4$, there is a distinguished 2-cycle of length 4 in this quadrangulation incident to out-directed edges from v (figure 4, see over). Let us denote this by $\partial Q(v)$ and the rest of $Q(v)$ as the interior of $Q(v)$. The cycle $\partial Q(v)$ divides $Q(v)$ into two parts both of which are quadrangulations.

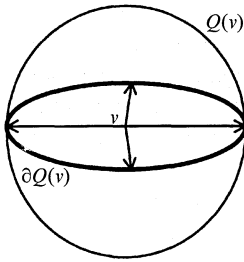


Figure 4. Configurations $Q(v)$ at vertex v , where $Q(v)$ is a quadrangulation embedded on a sphere, and $\partial Q(v)$ divides the quadrangulation into two parts.

Each edge in $Q(v)$ corresponds to a triangular face with v as the other vertex. There are no inward-directed edges from $\partial Q(v)$ because this would violate the condition that there are no triangular faces with a directed boundary. The vertices in the interior of $Q(v)$ have $\delta^+(v) = 2$, derived by means of counting arguments. Consequently, all the properties of directed quadrangulations corresponding to 2-rectangulations hold for each of the two parts of $Q(v)$, separated by the distinguished cycle. In particular, a cycle of length 4 in either part has no inward-directed edges (where the inside of the cycle does not contain the distinguished cycle).

The following construction identifies, for any vertex v in the interior of an octahedral map T in \mathcal{T} , an octahedral submap (having all 3-faces octahedra) which contains vertex v as an interior vertex. Let us take two vertices w_1 and w_2 of the same colour in $\partial Q(v)$ and consider $Q_1 = Q(w_1)$ and $Q_2 = Q(w_2)$. Let $Q_1 \cap Q_2$ be the vertex and edge intersection of Q_1 and Q_2 . Construct $C(v)$ with vertices reachable by paths from v (not necessarily directed) which do not cross ∂Q_1 or ∂Q_2 ; $C(v)$ is a quadrangulation with a boundary cycle of length 4 consisting of vertices and edges in ∂Q_1 or ∂Q_2 . Now construct $T(v)$ as the octahedral submap of T as generated by the vertices $\{C(v), w_1, w_2\}$. Further construct the octahedral submap $T'(v)$ [which includes all of $T(v)$] generated by vertices $\{Q_1 \cap Q_2, w_1, w_2\}$. In fact $T'(v) = T(v)$ because if there is vertex x in the boundary of $T(v)$ but interior to $T'(v)$ then 3-dimensional embedding prevents the construction of $T(x)$. Thus $C(v) = Q_1 \cap Q_2$. Note that $T(v)$ may enclose parts of T which are not part of $T(v)$.

Submap $T(v)$ has no in-directed edges from its boundary to an interior vertex. This is a general property of octahedral submaps of T . First, note that octahedral submaps of $T(v)$ have no in-directed edges. If T' is an octahedral submap of T and there is an edge from vertex x on the boundary of T' to an interior vertex y of T' , then construct $C(y)$ and the corresponding $T(y)$. The edge (x, y) is either an edge directed towards the interior of $T(y)$ or an inward-directed edge on a cycle of length 4. Both cases contradict the properties of $T(y)$. Thus: *An octahedral submap of an octahedral map in \mathcal{T} has no in-directed edges from its boundary to an interior vertex.*

This is analogous to the condition on cycles of length 4 in directed quadrangulations that there are no edges directed from the cycle towards its interior. However, note that for quadrangulations the result is established by counting arguments. In the three-dimensional case of octahedral maps, counting arguments only yield bounds on the numbers of inward-directed and outward-directed edges at the boundary of an octahedron. These are not strong enough to give useful properties of the octahedral submaps. It is necessary to consider explicitly the three-dimensional embedding of the maps.

We are now in position to show that: *The octahedral maps T are precisely the maximal plane adjacency maps of unlocked trivalent 3-rectangulations.*

This is established by induction on the number of vertices by using the construction of $T(v)$ at each vertex v . Note that each $T(v)$, when it has the edges of its boundary octahedron augmented so that they are bidirected, is a member of \mathbf{T} . Further, removing the interior of $T(v)$ [including vertices which do not belong to $T(v)$] leaves an octahedral map which is also in \mathbf{T} . A special case occurs when $T(v)$ contains the boundary octahedron. The interior quadrangulation is then constructed from a quadrangulation with fewer vertices with associated rules for construction of 2-rectangulations. The octahedral map with one interior vertex is the maximal plane adjacency map of a 3-rectangulation. Informally this means that an unlocked 3-rectangulation either has a sub-3-rectangulation or is a ‘thin’ rectangulation, one rectangle deep which has all the properties of a 2-rectangulation. The subrectangulation in turn satisfies the same property of having a sub-3-rectangulation or is a ‘thin’ rectangulation. These results indicate that unlocked trivalent 3-rectangulations are essentially two dimensional in character. An unlocked 3-rectangulation contains a subconfiguration which is an extruded 2-rectangulation. This means that 3-rectangulations can be viewed as a series of subdivisions of 3-rectangles by extruded 2-rectangulations. The three-dimensional complexity arises from application of the subdivision rule in three planes.

The submaps $T(v)$ have corresponding sub-3-rectangulations for each maximal plane in the rectangulation. The presence of these sub-3-rectangulations can be established directly from the geometric configuration of the maximal planes in rectangulations. We now present results on directed paths and cycles in directed octahedral maps in \mathbf{T} . These have direct parallels in 3-rectangulations and can be shown directly on the geometric configuration rather than by using the maximal plane adjacency map.

The construction of the octahedral submap $T(v)$ provides a way to establish results on directed 1-cycles in directed octahedral maps in \mathbf{T} . Suppose that vertex v belongs to a directed path P . If P leaves $T(v)$ then it cannot return to the interior of $T(v)$ because there are no in-directed edges. Thus if P leaves $T(v)$ it cannot be a cycle. Consider a 2-coloured directed cycle containing vertex v . As the cycle remains in $T(v)$ we have the general result: *A 2-coloured directed 1-cycle in an octahedral map in \mathbf{T} has all vertices adjacent to two vertices of the third colour by edges out-directed from vertices on the directed cycle.*

The consequences of the construction are stronger. Consider a 3-coloured path containing the vertex v in $T(v)$. The path must leave and cannot return to the interior of $T(v)$. Thus: *An octahedral map in \mathbf{T} has no 3-coloured directed cycles.*

By the construction of $T(v)$ its interior vertices form a directed quadrangulation. Thus, by the properties of directed quadrangulations, a directed 2-coloured path can always be found from the interior of $T(v)$ to the boundary of $T(v)$. A directed 2-coloured path from any vertex in an octahedral map \mathbf{T} leads to the boundary octahedron because the path repeatedly leaves octahedral submaps $T(v)$ and does not return. Thus: *There are 2-coloured directed paths (of each pair of colours) from each vertex of a map in \mathbf{T} to the boundary octahedron.*

The results for the directed octahedral maps \mathbf{T} can be interpreted directly for 3-rectangulations. The characteristics of directed 2-coloured cycles are straightforward to establish directly on 3-rectangulations. As a directed path passes from plane to plane, the ‘height’ of the plane increases. With a cycle these heights must all be equal and the planes in the cycle are all adjacent to a pair of planes orthogonal to those in the cycle. The result that there are no 3-coloured cycles is harder to establish directly and the maximal plane adjacency representation is an effective route to this result.

Generating 3-rectangulations

The methods of generation used above are based on suboctahedral maps or their corresponding subrectangulations. There are more straightforward generations based on the types of 3-rectangle present in a 3-rectangulation. The rules in figure 5 generate unlocked trivalent 3-rectangulations and depend on the fact that the right-hand sides of the rules represent the only two configurations for the planes around a rectangle. Thus, for any labelling r_1, r_2, \dots, r_n of the rectangles in a 3-rectangulation, there is an associated generation sequence which creates the rectangles in the same order r_1, r_2, \dots, r_n .

Other rules based on maximal plane configurations can be identified. These do not have the flexibility of those in figure 5 but are simpler in appearance. Suppose there are no directed cycles in an octahedral map in \mathcal{T} . There must be a vertex v with no in-directed edges. Thus v has four incident edges, all out-directed. On the other hand, if there is a directed cycle then this cycle lies on some quadrangulation $Q(v)$ adjacent to a vertex v . There is a directed cycle of length 4 from the results for directed quadrangulations. Thus each map T in \mathcal{T} has either a vertex of degree 4 or an octahedral face which has a directed cycle of length 4 on its boundary.

These results show that an element in \mathcal{T} can be generated by a sequence of operations which either add a vertex of degree 4 inside an octahedral face or split a vertex to create a new octahedral face. The 3-rectangulations are generated by the corresponding spatial compositions (figure 6). These generative results show that the

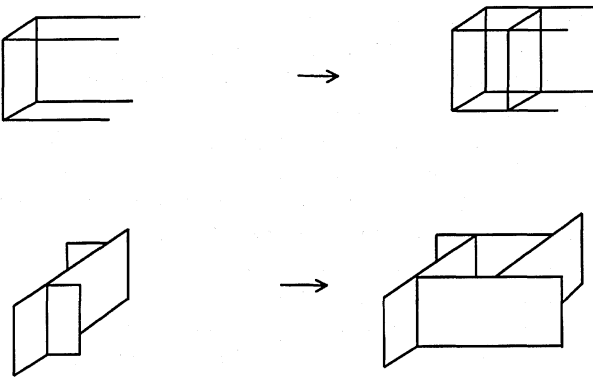


Figure 5. Rules for generating 3-rectangulations which can create component rectangles in any order.

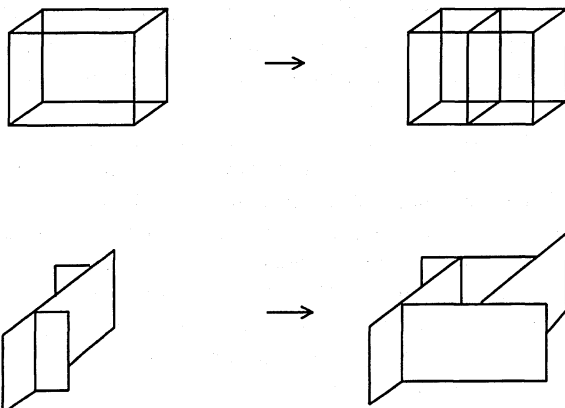


Figure 6. Rules for constructing 3-rectangulations.

unlocked trivalent 3-rectangulations are local variants of layered two-dimensional layouts. Unlocked 3-rectangulations are generated by rules which are extruded forms of the corresponding rules for 2-rectangulations. Three-dimensional variation is created by the three planes in which the local rules can be applied.

Descriptions of 3-rectangulations

The elements used to describe 3-rectangulations are maximal line and maximal plane elements in U_{13} and U_{23} , respectively. Selected volumes forming the 3-rectangles are appropriate for elements in U_{33} . Other plane elements form the segments which are maximal in the boundaries of volumes; other line elements are the boundaries of these plane segments. The description used here focuses on maximal planes and 3-rectangle volumes.

From these elements a closed shape description can be constructed. Let us select the following subshapes in $U_{03} \times U_{13} \times U_{23} \times U_{33}$ to describe a 3-rectangulation R : (1) 3-rectangle volumes including the overall bounding 3-rectangle; (2) plane boundaries of the 3-rectangles; (3) the line boundaries of these planes; and (4) the point boundaries of lines.

The 3-rectangulations are described as 3-rectangle volumes with the cumulative boundary, that is, the boundary planes, their boundary lines, and the boundary points of these lines. Unions and intersections of these shapes give further shapes which are volumes composed of several 3-rectangles and the associated planes and volumes. Intersections also include individual planes and lines (and their compositions). This set of subshapes includes fragmented pieces of boundary planes and forms a closure structure of closed shapes (Stiny, 1994). Closure $c(x)$ of a subshape x of a rectangulation R is the minimal closed shape containing the subshape.

The closure boundary (Earl, 1997) of a subshape x is the shape product $c(x)c(R-x)$ of the closure of x and of the shape complement $R-x$. A 3-rectangle volume x in R has closure; the shape consisting of x and its cumulative boundary of planes, lines, and points. The shape complements of $R-x$ are all planes, lines, and volumes, except x . The shape $R-x$ is closed because it comprises the sum of closed shapes. The closure boundary of x is thus the planes, lines, and points in its cumulative descriptive boundary. For subshape $x+y=z$ which is the sum of two 3-rectangle volumes x and y , the closure of shape z contains the boundary lines and planes of x and y . The shape complement $R-z$ is closed and the closure boundary of z is a cumulative descriptive boundary but not the minimal descriptive boundary. The closure of an arbitrary plane segment illustrates an interesting view of the closed sets which are planes (with their boundary lines). For two 3-rectangles in R adjacent via a plane, the plane segment shared by the two 3-rectangles is a closed shape. Thus, for an arbitrary plane segment x , the closure of x is the smallest closed plane segment containing x . This will not necessarily be the boundary plane of a 3-rectangle.

Other closed shapes consist of maximal planes and 3-rectangle volumes considered separately. These will include arbitrary collections of planes and volumes, without any boundary connection between them. There are many views of 3-rectangulations based on selections of subshapes and in terms of closed shapes. Allowing volumes, planes, and lines to be used independently in constructing descriptions creates rich and surprising views of 3-rectangulations. The restricted views of discrete volume elements packed together or of orthogonal maximal plane elements may constrain a wide-ranging exploration of possible designs in which these shapes are used. Describing 3-rectangulations in the product algebras helps to realise these possibilities.

Conclusion

Rectangulations are analysed in terms of shape descriptions. Shape elements and their relations provide multiple descriptions. One of these descriptions, the maximal element adjacency, is used as the basis of a formal representation. The configurations of maximal lines and maximal planes in densely packed rectangulations are described by embedded maps representing adjacencies of these spatial elements. We identify exactly which maps are descriptions of densely packed rectangulations. These descriptions are used to determine properties of densely packed rectangulations as well as methods of generation. Some of these results are derivable directly from the geometric configuration without the mediation of the representation.

In this paper we have shown that 3-rectangulations with constraints on neighbouring rectangles defined by unlocked and trivalent joints form three-dimensional layouts which are 'local' variants of 'layered' two-dimensional layouts. There are two ways in which this interpretation arises, generatively and configurationally.

We conclude that the unlocked 3-rectangulations described here still maintain an essentially two-dimensional structure. It is necessary to examine locked 3-rectangulations to observe complex three-dimensional behaviour. The representation of locked 3-rectangulations and the consequent derivation of their spatial properties requires more powerful methods than those presented here. However, distinguishing these two categories of spatial configuration allows us to identify the limits of current representations and the extent of the complexity of three-dimensional spatial arrangements.

References

- Bondy J A, Murty U S R, 1976 *Graph Theory with Applications* (Macmillan, London)
- Brown W, 1965, "Enumeration of quadrangular dissections of the disk" *Canadian Journal of Mathematics* **17** 302 – 317
- Cagan J, Mitchell W J, 1993, "Optimally directed shape generation by shape annealing" *Environment and Planning B: Planning and Design* **20** 5 – 12
- Campbell M I, Amon C H, Cagan J, 1997, "Optimal three-dimensional placement of heat generating electronic components" *ASME Journal of Electronic Packaging* **119**(2) 106 – 113
- Chao K, Guenov M, Hills W, Smith P, Buxton I, Tsai C, 1997, "An expert system to generate associativity data for layout design" *Artificial Intelligence in Engineering* **11** 191 – 196
- Choi B, Flemming U, 1996, "Adaptation of a layout design system to a new domain: construction site layouts", in *Proceedings of the 3rd Congress on Computing in Civil Engineering (III-CCCE)*, Anaheim, CA, June 17 – 19, Eds J Vanegas, P Chinowsky, American Society for Civil Engineers, 1801 Alexander Bell Drive, Reston, VA 20191-4400, pp 711 – 717
- Earl C F, 1978, "Joints in two and three dimensional rectangular dissections" *Environment and Planning B* **5** 179 – 187
- Earl C F, 1980, "Rectangular shapes" *Environment and Planning B* **7** 311 – 342
- Earl C F, 1997, "Shape boundaries" *Environment and Planning B: Planning and Design* **24** 669 – 687
- Flemming U, 1978, "Wall representations of rectangular dissections and their use in automated spatial allocation" *Environment and Planning B* **5** 215 – 232
- Flemming U, 1980, "Wall representations of rectangular dissections: additional results" *Environment and Planning B* **7** 247 – 251
- Flemming U, 1986, "On the representation of loosely packed arrangements of rectangles" *Environment and Planning B: Planning and Design* **13** 189 – 205
- Flemming U, 1989, "More on the representation and generation of loosely packed arrangements of rectangles" *Environment and Planning B: Planning and Design* **16** 327 – 359
- Flemming U, Baykan C A, Coyne R F, Fox M S, 1992, "Hierarchical generate-and-test vs. constraint-directed search. A comparison in the context of layout synthesis", in *Artificial Intelligence in Design '92* Ed. J Gero (Kluwer, Dordrecht) pp 817 – 838
- Flemming U, Chien S F, 1995, "Schematic layout design in SEED environment" *ASCE Journal of Architectural Engineering* **1** 162 – 169
- Hicks C, Earl C F, Hinrichs J, 1994, "Integration of layout and clustering techniques with discrete event simulation of a manufacturing environment", in *Proceedings of the European Simulation Symposium Istanbul*, 9 – 12 October, Eds A Kaylan, A Lehrmann, T Owen; Society for Computer Simulation International, PO Box 17900, San Diego, CA 92177-7900

-
- Krishnamurti R, 1979, "3-rectangulations: an algorithm to generate box packings" *Environment and Planning B* **6** 331 – 352
- Krishnamurti R, 1993, "Dense 3-rectangular arrangements", working paper, Department of Architecture, Carnegie Mellon University, Pittsburgh, PA
- Kundu S, 1988, "The equivalence of the subregion representation and the wall representation for a certain class of rectangular dissections" *Communications of ACM* **31** 752 – 763
- Preas B T, Cleemput W M van, 1979, "Placement algorithms for arbitrary shaped blocks", in *Proceedings of the 16th Design Automation Conference* Association for Computing Machinery, 1133 Avenue of the Americas, New York, NY10036; reprinted 1988 in *25 Years of Electronic Design Automation: The Most Influential Papers* ACM, New York, pp 199 – 205
- Smith N, Hills W, Cleland G, 1996, "Parallel implementation of simulated annealing for layout design using speculative computation" *Journal of Engineering Design* **7** 363 – 375
- Steadman J P, 1983 *Architectural Morphology* (Pion, London)
- Stiny G, 1991, "The algebras of design" *Research in Engineering Design* **2** 171 – 181
- Stiny G, 1994, "Shape rules: closure, continuity and emergence" *Environment and Planning B: Planning and Design* **21** s49 – s78
- Stouffs, 1994 *The Algebras of Shapes* PhD thesis, Department of Architecture, Carnegie Mellon University, Pittsburgh, PA
- Supowit K J, Slutz E A, 1984, "Placement algorithms for VLSI" *Computer Aided Design* **16**(1) 45 – 50
- Szykman S, Cagan J, 1995, "A simulated annealing-based approach to three-dimensional component packing" *ASME Journal of Mechanical Design* **117**(2) 308 – 314
- Szykman S, Cagan J, 1997, "Constrained three-dimensional component layout using simulated annealing" *ASME Journal of Mechanical Design* **119**(1) 28 – 35